Neuro-Oncology
24(7), 1150–1163, 2022 | https://doi.org/10.1093/neuonc/noab300 | Advance Access date 29 December 2021

Dual IGF1R/IR inhibitors in combination with GD2-CAR T-cells display a potent anti-tumor activity in diffuse midline glioma H3K27M-mutant

Emmanuel de Billy, Marsha Pellegrino, Domenico Orlando, Giulia Pericoli, Roberta Ferretti, Pietro Businaro, Maria Antonietta Ajmone-Cat, Sabrina Rossi, Lucia Lisa Petrilli, Nicola Maestro, Francesca Diomedi-Camassei, Marco Pezzullo, Cristiano De Stefanis, Paola Bencivenga, Alessia Palma, Rossella Rota, Francesca Del Bufalo, Luca Massimi, Gerrit Weber, Chris Jones, Andrea Carai, Simona Caruso, Biagio De Angelis, Ignazio Caruana, Concetta Quintarelli, Angela Mastronuzzi, Franco Locatelli†, and Maria Vinci†

Department of Onco-hematology, Gene and Cell Therapy, Bambino Gesù Children's Hospital–IRCCS, Rome, Italy (E.D.B., M.P., D.O., G.P., R.F., P.B., L.L.P., N.M., R.R., F.D.B., G.W., S.C., B.D.A., I.C., C.Q., A.M., F.L., M.V.); National Centre for Drug Research and Evaluation, Istituto Superiore di Sanità–Rome, Rome, Italy (M.A.A.C.); Department of Laboratories-Pathology Unit, Bambino Gesù Children's Hospital-IRCCS, Rome, Italy (S.R., F.D.C.); Research Laboratories, Bambino Gesù Children's Hospital-IRCCS, Rome, Italy (M.P., C.D.S., P.B., A.P.); Department of Pediatric Neurosurgery, Catholic University Medical School, Rome, Italy (L.M.); Division of Molecular Pathology, Institute of Cancer Research, Sutton, UK (C.J.); Department of Neuroscience and Neurorehabilitation, Bambino Gesù Children's Hospital-IRCCS, Rome, Italy (A.C.); Department of Clinical Medicine and Surgery, University of Naples Federico II, Naples, Italy (C.Q.); Department of Pediatrics, Sapienza University of Rome, Rome, Italy (F.L.)

†Shared last authorship.

Corresponding Authors: Emmanuel de Billy, PhD, Department of Onco-Hematology, Gene and Cell Therapy, Bambino Gesù Children's Hospital–IRCCS, viale San Paolo 15, 00146, Rome, Italy (emmanuel.decrespin@opbg.net); Franco Locatelli, MD, PhD, Department of Onco-Hematology, Gene and Cell Therapy, Bambino Gesù Children's Hospital–IRCCS, viale San Paolo 15, 00146, Rome, Italy (franco.locatelli@opbg.net); Maria Vinci, PhD, Department of Onco-Hematology, Gene and Cell Therapy, Bambino Gesù Children's Hospital–IRCCS, viale San Paolo 15, 00146, Rome, Italy (maria.vinci@opbg.net).

Abstract

Background. Diffuse midline gliomas (DMG) H3K27M-mutant, including diffuse intrinsic pontine glioma (DIPG), are pediatric brain tumors associated with grim prognosis. Although GD2-CAR T-cells demonstrated significant anti-tumor activity against DMG H3K27M-mutant in vivo, a multimodal approach may be needed to more effectively treat patients. We investigated GD2 expression in DMG/DIPG and other pediatric high-grade gliomas (pHGG) and sought to identify chemical compounds that would enhance GD2-CAR T-cell anti-tumor efficacy.

Methods. Immunohistochemistry in tumor tissue samples and immunofluorescence in primary patient-derived cell lines were performed to study GD2 expression. We developed a high-throughput cell-based assay to screen 42 kinase inhibitors in combination with GD2-CAR T-cells. Cell viability, western blots, flow-cytometry, real time PCR experiments, DIPG 3D culture models, and orthotopic xenograft model were applied to investigate the effect of selected compounds on DIPG cell death and CAR T-cell function.

Results. GD2 was heterogeneously, but widely, expressed in the tissue tested, while its expression was homogeneous and restricted to DMG/DIPG H3K27M-mutant cell lines. We identified dual IGF1R/IR antagonists, BMS-754807 and linsitinib, able to inhibit tumor cell viability at concentrations that do not affect CAR T-cells. Linsitinib, but not BMS-754807, decreases activation/exhaustion of GD2-CAR T-cells and increases their central memory profile. The enhanced anti-tumor activity of linsitinib/GD2-CAR T-cell combination was confirmed in DIPG models in vitro, ex vivo, and in vivo.

Conclusion. Our study supports the development of IGF1R/IR inhibitors to be used in combination with GD2-CAR T-cells for treating patients affected by DMG/DIPG and, potentially, by pHGG.

Key Points

- GD2 is heterogeneously expressed in patient DMG/DIPG and pHGG tumor tissue.
- IGF1R/IR inhibitors synergize with GD2-CAR T-cell therapy in DMG/DIPG.

Importance of the Study

Our study is the first to demonstrate that GD2 is heterogeneously but widely expressed in DMG/DIPG and pHGGs tissue samples. We also demonstrate the therapeutic potential of targeting IGF1R/IR in combination with GD2-CAR T-cells to improve anti-tumor efficacy. In particular, the dual IGF1R/IR inhibitor linsitinib increases tumor cell death and enhances GD2-CAR T-cells anti-tumor activity providing a strong rationale for future translational development of IGF1R/IR inhibitor as adjuvant of GD2-CAR T-cells therapy for DMG/DIPG and potentially other pHGGs.

Diffuse midline gliomas (DMG), including diffuse intrinsic pontine glioma (DIPG), are aggressive tumors of the central nervous system (CNS) affecting children and adolescents, with a median overall survival shorter than 1 year.[1,2] These tumors occur in the midline regions of the brain, including the thalamus, the midbrain, and the pons.

DMG/DIPG are largely characterized by recurrent somatic mutations in genes encoding histone H3.3 and H3.1 variants, with the most common substitution of lysine to methionine at position 27 (H3K27M).[3,4] Given the strong association of the H3K27M mutations with the midline tumors, the World Health Organization (WHO) defined the new tumor entity as DMG H3K27M-mutant.[5] In addition to the K27M mutation, other alterations such as overexpression of EZHIP and alterations in EGFR,[6] can define this entity. Therefore, in the latest 2021WHO classification of CNS tumors, these lesions are now defined as DMG H3 K27-altered.[7] The identification of the other recurrent somatic mutations such as the glycine or valine to arginine substitutions at the position 34 of the histone variant H3.3 (H3.3G34R/V),[3,4] has led to the definition of a new entity, Diffuse hemispheric glioma, H3 G34-mutant.[7]

DMG/DIPG are often inoperable, in particular the pontine tumors, chemo-resistant, and only transiently controlled by radiotherapy.[8] Despite numerous collaborative studies and clinical trials,[9] patient survival has not significantly improved over the last 30 years, making DMG/DIPG one of the biggest therapeutic challenge in pediatric oncology. One reason for the lack of therapeutic efficacy is linked to the high degree of genetic and phenotypic heterogeneity observed in DIPG.[10]

A recent preclinical study suggested that the immunotherapeutic approach using a GD2 re-directed Chimeric Antigen Receptor (CAR)-expressing T-cell (GD2-CAR T-cell), might be beneficial for DMG/DIPG.[11] More recently, CAR T-cells targeting different antigens have shown anti-tumor activity in mice grafted with pediatric brain tumor cells, with limited signs of neurologic, or systemic toxicity.[12,13] However, success of GD2-CAR T-cell therapy for DMG/DIPG could be hampered by malignant cells escaping from the lytic effect of CAR T-cells, and by the possible occurrence of a neuroinflammatory reaction leading to unacceptable toxicity.[11] Another potential restricting factor is the immune-cold microenvironment characterizing DMG H3K27M-mutant.[14] While the immune-cold microenvironement may have a positive impact by preventing the infiltration of immunosuppressive cells, it may also predict a limited recruitment and infiltration of CAR T-cells.[15] Altogether, these observations indicate the need to implement the current CAR T-cell therapeutic strategies to more efficiently and safely treat young patients affected by this disease.

Different approaches are under development to improve CAR T-cell-based immunotherapeutic activity against solid tumors. These include improving the persistence, expansion, activation, and homing of the immune cells by adding different costimulatory domains in the CAR molecule,[16] or by genetic modification of different T-cell surface receptors or secreted factors.[17] Other strategies consist of combining CAR T-cells with either monoclonal antibodies to target inhibitory immune checkpoints, or oncolytic virus or small chemical molecules to increase tumor cell death and improve CAR T-cell efficacy.[18,19]

Among the different approaches, chemical drugs may present an advantage by acting in concert with the engineered T-cells, either by inhibiting tumor cell proliferation, or potentiating the intrinsic CAR T-cell activity, or by displaying both effects simultaneously.[18] Several combination studies using small molecules targeting specific oncogenic signaling pathways have been tested in vitro or in preclinical models for different tumor types.[18] However, modulation of the immune and anti-tumor activities of the T-cells observed in response to small chemical agents may vary depending on the tumor type and localization, its genetic background, tumor microenvironment (TME), and CAR specificity.[20] Based on these observations, we hypothesized that chemical drugs, in combination with

GD2-CAR T-cells, could improve the treatment efficacy of patients affected by DMG/DIPG.

In this study, after having investigated GD2 expression in DMG/DIPG and other pHGGs, we developed a high-throughput cell-based screening assay to identify small molecules able to potentiate GD2-CAR T-cell activity. The screen led to the identification of the dual IGF1R/IR antagonists as adjuvants of GD2-CAR T-cell activity for treatment of DMG H3K27M-mutant and potentially of other HGG.

Materials and Methods

Patient Tissue Samples

Patient tissues and blood samples were collected in accordance with the rules of the Institutional Ethical Committee of the Bambino Gesù Children's Hospital (Ethical Committee Approvals N°1343/2018; N°969/2015; N°1952/2019) and with the Helsinki Declaration and its later amendments or comparable ethical standards; written informed consent was obtained by patient's legal guardians.

Histology and Immunohistochemistry

Paraffin embedded patient tissue samples were immunostained with antibodies against Histone H3K27M, Histone H3.3G34R, GD2, IGF1R, and Pospho-IGF1R (P-IGF1R), as detailed in the Supplementary Material.

Cell Lines and Culture Conditions

Primary patient-derived cell lines were derived as previously described.[21] Cell authenticity and mycoplasma test were performed. Experimental details are outlined in the Supplementary Material.

Immunofluorescence Assay

Cells were seeded on laminin-coated 96-well plates (ViewPlate-96, PerkinElmer) and fixed with 4% paraformaldehyde. For GD2 staining, cells were incubated with an anti-Human GD2 PE-conjugated antibody. For histone staining, cells were incubated with an anti-Human H3K27M mutant and with an anti-human H3.3G34R antibodies. Images were acquired with a 20× objective using the Operetta CLS™ (PerkinElmer). Experimental details are in the Supplementary Material.

T-Cell Transduction

Transduction of the GD2-CAR.CD28.4-1BB. ζ construct was performed as previously described.[16,22] Experimental procedures are reported in the Supplementary Material.

Flow-Cytometry Assay

Flow cytometry analysis was performed on a BD LSRFortessa X-20 (BD Biosciences) for the detection of GD2, H3K27M, IGF1R, IR, CD3, and for T-cell phenotype, as described in the Supplementary Material. FACS Diva software (BD Biosciences) was used for data analysis taking into account 10,000 events/experiment.

Cell Transduction for Enhanced Green Fluorescence Protein (eGFP) Expression

Five-thousand SU-DIPG-VI cells/well were seeded into a laminin-coated 24-well plate (Corning) in Tumor Stem-cell Medium (TSM). Retroviral cell transduction was performed using the retrovirus previously described[23] encoding for eGFP-Firefly-Luciferase as described in the Supplementary Material.

Screening and Viability Assays

For the screening assay, 12,000/well DIPG cells were seeded onto laminin-coated 96-well plates (ViewPlate-96 Black) and incubated with compounds (Supplementary Table 1) at 1 μM for 1 h before the addition of GD2-CAR or nontransduced (NT) T-cells. Brightfield live cell images were acquired at the OperettaCLS (PerkinElmer) and analyzed with Harmony Software 4.8 (PerkinElmer) as described in Figure 2A. Details of the experimental procedures are in the Supplementary Material.

Western Blot Assay

Western blot analysis was performed following standard procedures. Primary antibodies were incubated overnight at 4°C and secondary antibodies (horseradish HRP-conjugated, Thermofisher) were incubated for 1 h at RT. Proteins were revealed using enhanced chemiluminescence Immobilon Western Chemiluminescent HRP Substrate (Millipore) and images acquired with ChemiDoc Imaging Systems (BIORAD). Experimental details are in the Supplementary Material.

RNA Extraction and Quantitative PCR

RNA isolation and PCR experimental details are reported in the Supplementary Material.

3D Experiments

SU-DIPG-VI-eGFP$^+$ neurospheres (NS) were generated in 96-well round-bottom plates ULA (Corning), treated with 5 μM of linsitinib or DMSO vehicle control in presence or absence of CAR T-cells for 24 h. Upon incubation with propidium iodide (PI), live image-analysis was performed using the Celigo cytometer (Nexcelom). In an additional set of experiments, CAR T-cells were labeled with PKH26 and cocultured with DIPG NS as described above. Image analysis was performed at the Operetta CLS™. Experimental details are in the Supplementary Material.

Whole Brain Organotypic Slice

Whole brain organotypic slices (WBOS) were prepared and cocultured with DIPG NS as previously described.[21]

Experimental details including treatment, staining, and image analysis are reported in the Supplementary Material.

In Vivo Orthotopic Xenograft Model

A detailed description of the in vivo experiments is reported in the Supplementary Material.

All animal experiments were in accordance with the European Communities Council Directive N. 2010/63/EU, the Italian Ministry of Health guidelines (DL 26/2014), and approved by the Italian Ministry of Health and the local Institutional Animal Care and Use Committee (IACUC) at Istituto Superiore di Sanità (Rome; protocol n. D9997.N.BYG and n° 1048/2020-PR).

DNA Extraction and Sanger Sequencing

DNA extraction and sanger sequencing for the histone mutations was performed as previously described.[21] Primer sequences are in Supplementary Table 2.

Statistical Analysis

Data are reported as mean ± standard deviation (SD) and statistical analysis performed with GraphPad Prism 6 software. For the screening assay, statistical significance was evaluated using unpaired, two-tailed t-test while for 2D/3D/WOBS statistical significance was evaluated with One-way ANOVA and Bonferroni's Multiple Comparison Tests. For T-cell profiling, statistical significance was evaluated with the Paired t-test. Throughout the study ****$P < .0001$; ***$P < .001$; **$P < .01$; *$P < .05$; ns: nonsignificative.

Results

GD2 Expression is Not Limited to DIPG/DMG H3K27M-Mutant

Mount et al.[11] recently demonstrated GD2 expression in DMG H3K27M-mutant. To confirm and extend these findings, we investigated GD2 expression by immunohistochemistry (IHC) in tissue samples from 9 patients, including three DMG H3K27M-mutant, two Diffuse hemispheric glioma H3 G34-mutant, and four Diffuse pediatric-type high-grade glioma, H3 wild-type, IDH wildtype[7] (Figure 1A, Supplementary Figure 1, Table 1 and Supplementary Tables 3 and 4).

We confirm GD2 expression in both histone H3.3 and H3.1K27M positive DMG/DIPG tumors but we also observed its expression in other pHGGs, histone WT, or carrying the H3.3G34R mutation (Figure 1A and Supplementary Figure 1A). The GD2 staining was cytoplasmic and/or nuclear, focal, or diffuse, showing a varying intensity from mild to strong, and this heterogeneity was observed independently of the tumor locations and molecular subgroups (Table 1 and Supplementary Table 4).

Furthermore, the nonneoplastic tonsil was negative for GD2, confirming the specificity of our staining, and in agreement with previous findings,[24] focal cytoplasmic GD2 staining was observed in some cortical neurons of the normal cortex, while the perineural oligodendrocyte was negative (Supplementary Figure 1B).

Using primary cell lines derived from the tumor tissue samples described in Figure 1A we found that GD2 is expressed in the DMG/DIPG cells, irrespective of their H3.3K27M or H3.1K27M mutational status, while is not expressed in pHGG H3.3G34R-mutant and histone WT cell lines (Figure 1B and Supplementary Figure 2). Notably, GD2 and H3K27M expression patterns were homogenous, as demonstrated by flow-cytometry analysis (Supplementary Figure 3).

Screening Kinase Inhibitors to Identify Modulators of GD2-CAR T-Cell Activity

Following our GD2 expression data, we selected a H3K27M-mutant cell line to develop a high-throughput cell-based assay to identify compounds that would potentiate CAR T-cell anti-tumor activity in DMG/DIPG. The OPBG-DIPG002 cells were cocultured with GD2-CAR T-cells for 24 h and live cell images were acquired and analyzed. Based on the differences in morphology and texture between DIPG cells and the floating DIPG/CAR T-cell aggregates, we specifically determined cell confluency (Figure 2A). Compared to the nontransduced (NT) T-cell, increasing the number of GD2 CAR T-cells led to a decrease in tumor cell confluency and to an increase in the cell aggregates (Figure 2B and C), confirming the relation between cell confluency and GD2-CAR T-cell cytotoxic activity. The assay was robust with a Z′ factor > 0.6 suitable for cell-based screening.

We screened 42 kinase inhibitors following the workflow described (Figure 2D). Hits were defined as compounds that at 1 μM and in combination with GD2-CAR T-cells, significantly decreased tumor cell confluency by 10% when compared to GD2-CAR T-cell treatment alone (Figure 2E). Eight compounds, including PI3Ks (NVP-BGT226, Omipalisib), AKT (Ipatasertib), PAN CDK (Dinaciclib), and a selective CDK2 (AUZ 454), as well as a C-MET (Tivantinib), ALK (Ensartinib), and a dual IGF1R/IR (BMS-754807) kinase inhibitors, were selected. Among those, only NVP-BGT226 and Omipalesib significantly increased and decreased, respectively the confluency of the aggregated cells suggesting that they could differentially affect CAR-T cell activity. To eliminate compounds toxic to T-cells or with general toxic activity on both tumor and T-cells, we looked at their treatment effect on the viability of OPBG-DIPG002 and GD2-CAR T-cells separately.

After 24 h of incubation and at the concentration of 1 μM, Dinaciclib, and NVP-BGT226 strongly affected both DIPG and GD2-CAR T-cell viability and were discarded (Figure 2F and G). The 6 remaining compounds showing no or minimal effect on CAR T-cell viability and strong to moderate activity on DIPG cells, were further investigated by performing dose-response assays to determine the concentration of compound that induced a 50% inhibition of cell proliferation (GI50) after 96h (Supplementary Table 5). The PI3K, AKT, as well as CDK2, C-MET, and ALK inhibitors were discarded, being equipotent on both cell types or more potent at inhibiting GD2-CAR T-cell. Interestingly, the dual

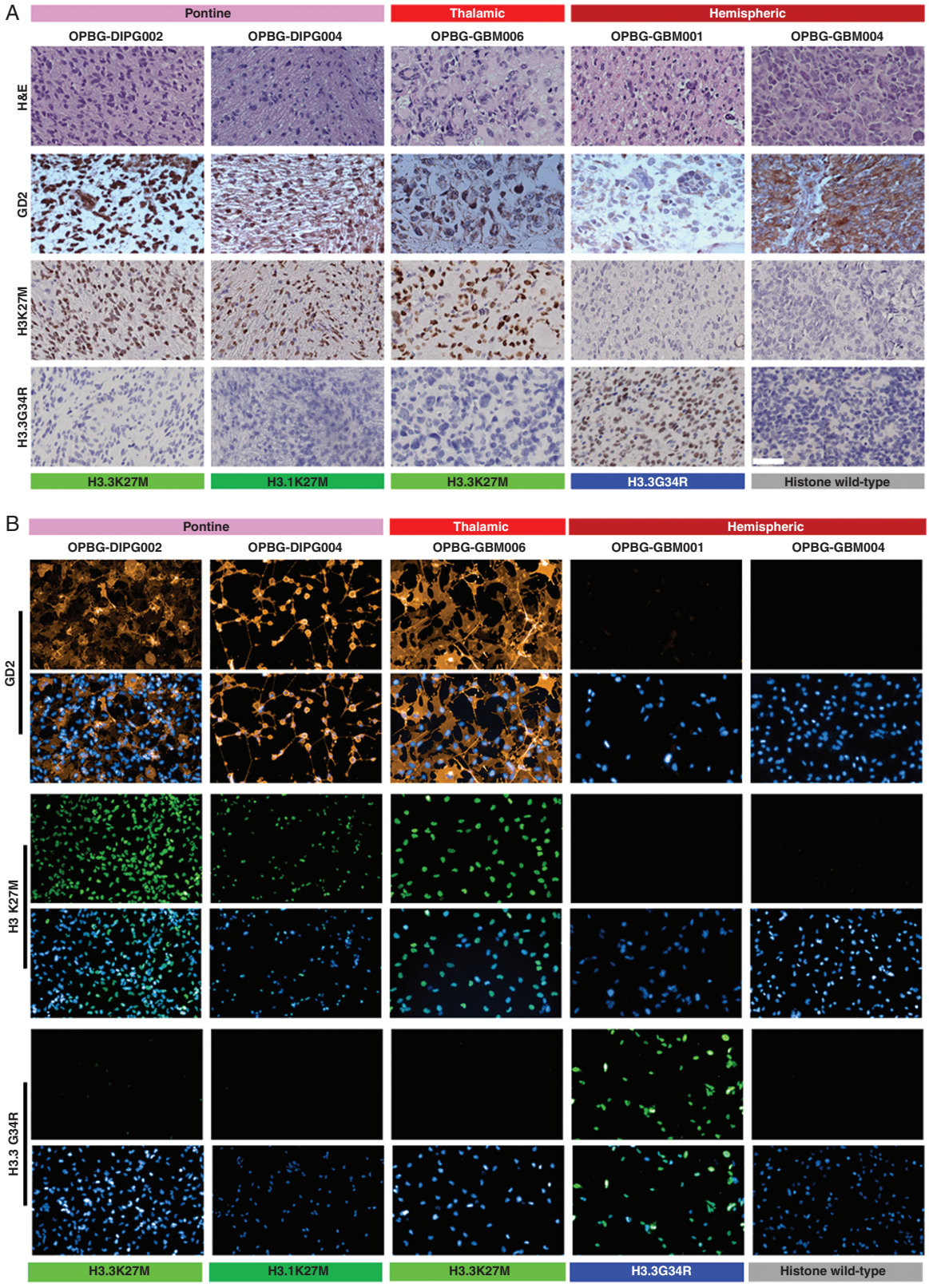

Fig. 1 GD2 expression in DMG/DIPG and pHGG patient tumor tissue samples primary-derived cell lines. (A) Representative images (40×) of tumor tissue samples stained for H&E and immunostained for GD2, H3K27M, and H3.3G34R. Scale bar = 50 μm. (B) Representative immunofluorescence images of primary patient-derived cell lines immunostained for GD2, H3K27M, and H3.3G34R. DAPI was used for nuclear staining. Scale bar = 100 μm. Tumor location and histone status are indicated.

Table 1 Summary of GD2 Expression in Tumor Tissue Samples

Patients	Sample code	Diagnosis	Histone status	Cytoplasmatic		Nuclear	
				Pattern	Intensity	Pattern	Intensity
1	OPBG-DIPG002	Diffuse midline glioma, H3 K27-altered	H3K27M	Focal	++	Diffuse	+++
2	OPBG-DIPG004 biopsy	Diffuse midline glioma, H3 K27-altered	H3K27M	Diffuse	+	Diffuse	++
	OPBG-DIPG004 autopsy		H3K27M	Diffuse	++	Diffuse	+++
3	OPBG-GBM006	Diffuse midline glioma, H3 K27-altered	H3K27M	Focal	+	Focal	++
4	OPBG-GBM001	Diffuse hemispheric glioma, H3 G34-mutant	H3.3G34R	Diffuse	+	No staining	
5	OPBG-GBM004	Diffuse pediatric-type high-grade glioma, H3 wildtype, and IDH wildtype	WT	Diffuse	++	Focal	+
6	OPBG-5299	Diffuse hemispheric glioma, H3 G34-mutant	H3.3G34R	Diffuse	+	Focal	++
7	OPBG-4402	Diffuse pediatric-type high-grade glioma, H3 wildtype, and IDH wildtype	WT	No staining		Diffuse	++
8	OPBG-3200	Diffuse pediatric-type high-grade glioma, H3 wildtype, and IDH wildtype	WT	Diffuse	+	No staining	
9	OPBG-0216	Diffuse pediatric-type high-grade glioma, H3 wildtype and IDH-wildtype	WT	Diffuse	++	Diffuse	++

IGF1R/IR kinase inhibitor, BMS-754807 (BMS), was 20 folds more effective at inhibiting DIPG cells than GD2-CAR T-cells proliferation. Based on this difference in activity, BMS was chosen for further investigations.

Dual IGF1R/IR Antagonists in Combination with GD2-CAR T-Cells affect DIPG Cell Proliferation

To confirm the enhanced anti-tumor effect of the BMS/GD2-CAR T-cell combination, we used BMS at the concentration of 0.75 μM corresponding to 5 times the GI50 value obtained on OPBG-DIPG002 cells. A significant decrease in DIPG cell confluency, indicative of an increase in cell death, was observed in the BMS/GD2-CAR T-cell cotreated samples, when compared to their use as single agents and to BMS in combination with the NT T-cells (Figure 3A). Similar results were obtained with GD2-CAR T-cells generated from two additional donors (Supplementary Figure 4A).

BMS is a poorly selective compound known to inhibit other kinases beside IGF1R/IR.[25] Thus, we tested the sensitivity of OPBG-DIPG002 and GD2-CAR T-cells in response to compounds targeting the off-targets of BMS. These included linsitinib (LIN), another IGF1R/IR antagonist, which was the only compound to show a differential sensitivity between OPBG-DIPG002 and GD2-CAR T-cells, comparable to BMS (Supplementary Table 6). Similar to BMS, LIN in combination with GD2-CAR T-cells decreased OPBG-DIPG002 cell confluency (Figure 4B). Both IGF1R/IR inhibitors in combination with GD2-CAR T-cells, showed similar effect on two additional DIPG cell lines, SU-DIPG-VI[11] and OPBG-DIPG004 (Supplementary Figure 4B and C).

DIPG, But Not GD2-CAR T-Cells, Express IGF1R and IR Proteins

Next, we characterized the IGF1R/IR pathway in the DIPG and GD2-CAR T-cells. Western blot analysis revealed that IGF1R and IR proteins were not detected in GD2-CAR T-cells, while they were expressed in the three DIPG cell lines tested (Figure 4C) with IGF1R phosphorylated at Tyr1135, indicating pathway activation. IHC analysis confirmed a diffuse expression of IGF1R and a more heterogeneous expression of P-IGF1R in patient tissue samples (Supplementary Figure 5).

The DIPG cell lines were equally sensitive to both antagonists after 96 h of treatment (Figure 3D and E) in contrast to GD2-CAR T-cells, less sensitive to both IGF1R/IR kinase inhibitors. BMS inhibited CAR T-cell viability at a concentration above 0.75 μM, potentially due to off-target effects, while LIN treatment did not, up to 5 μM.

Furthermore, we evaluated BMS and LIN treatment effects on the protein expression and phosphorylation of IGF1R and its downstream effector AKT (Figure 3F and G). Phosphorylation of STAT3, a player in the regulation of T-cell activity, and of ERK, were also investigated. A dose-dependent inhibition of IGF1R and AKT protein phosphorylation was observed in DIPG cells. As expected, no modulation of AKT protein and its phosphorylation was observed in CAR T-cells. Moreover, no variation in ERK and STAT3 protein and phosphorylation were seen in both cell types.

Altogether, these results clearly indicate that DIPG cells are sensitive to IGF1R/IR kinase inhibitors and that these agents can be used in combination with GD2-CAR T-cells.

Linsitinib and BMS-754807 Differently Modulate GD2-CAR T-Cell Phenotypes

Despite no effect on the viability and absence of IGF1R/IR expression, we could not exclude that the two antagonists would affect the CAR T-cell phenotype and function. We looked first at the effect of both inhibitors on IFNγ and TNFα mRNA expression, normally induced in antigen-activated T-cells, as shown upon activation with the anti-GD2-CAR

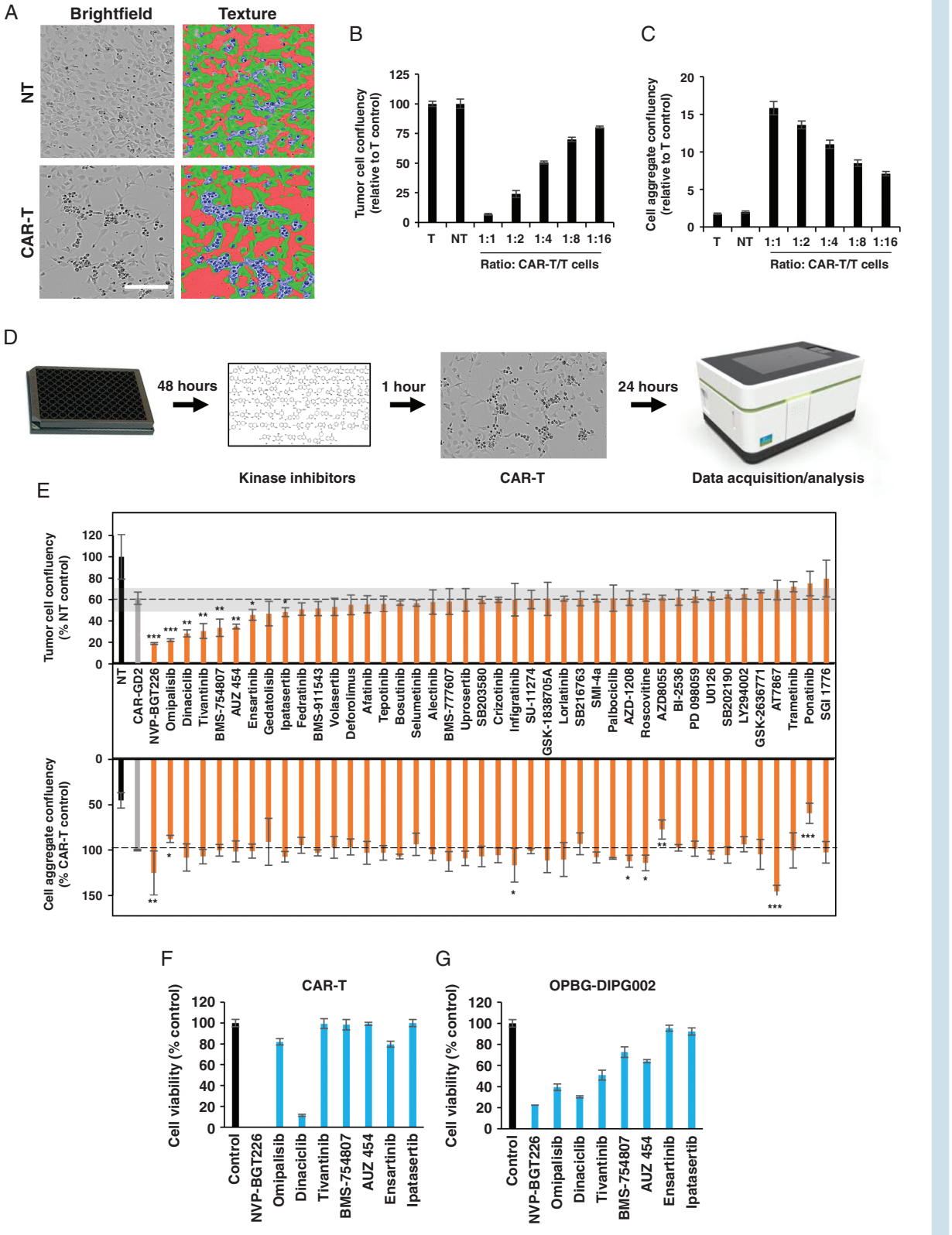

Fig. 2 Drug screening to identify modulators of GD2-CAR T-cells anti-tumor activity. (A) Brightfield images of OPBG-DIPG002 cells cocultured with CAR-T or (NT T-cells acquired and analyzed with Operetta CLS. DIPG cells (green), aggregated cells (blue), and empty space (red) are segmented. Scale bar = 100 μm. (B–C) Confluency quantification for OPBG-DIPG002 (B) and aggregated cells (C) in different CAR T-cells/DIPG cell ratios. (D) High-throughput cell-based assay workflow. (E) Results of the drug screen performed with 42 kinase inhibitors: Tumor (upper panel) and aggregated cell (lower panel) confluency. The 10% cutoff is indicated in gray. (F–G) Cell viability of CAR T-cells (F) and OPBG-DIPG002 cells (G) after 24 h of incubation with compounds at 1 uM. Results are mean ± SD of $n = 3$.

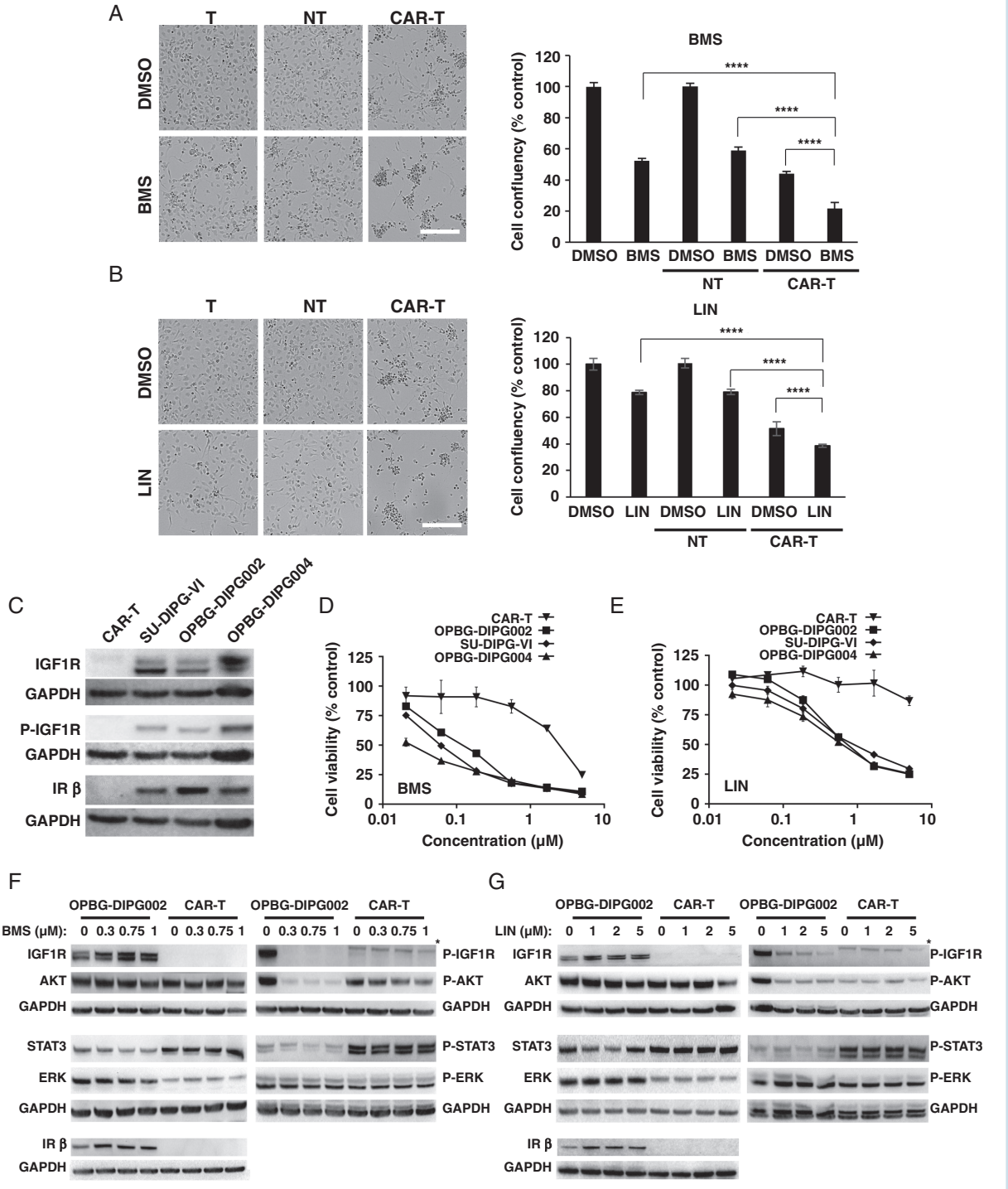

Fig. 3 IGF1R/IR pathway inhibition affects DIPG, but not GD2-CAR T-cells. (A–B) Brightfield images and corresponding cell confluency quantification of OPBG-DIPG002 cells treated with BMS (A) (0.75 μM) or LIN (B) (5 μM) alone and with CAR or NT T-cells. DMSO was used as vehicle control. Scale bar = 100 μm. (C) Western blot analysis of the indicated protein in DIPG and CAR T-cells. (D–E) Dose-response curves for BMS and LIN with the indicated cells. Results are mean ± SD from 1 representative of 3 experiments; $n = 3$ replicates. (F–G) Western blot analysis for the indicated proteins in OPBG-DIPG002 and CAR T-cells treated with BMS (F) or LIN (G). *nonspecific signal.

idiotype 1A7 antibody (Figure 4A). While BMS did not attenuate T-cell activation, LIN led to a significant decrease in IFNγ and TNFα mRNA levels suggesting that the two IGF1R/IR antagonists have differences in their modes of action.

Therefore, we investigated the effect of both antagonists on activation, exhaustion, and memory phenotype of T cells. For this purpose, either GD2-CAR or NT T-cells were incubated with the IGF1R/IR antagonists or DMSO as

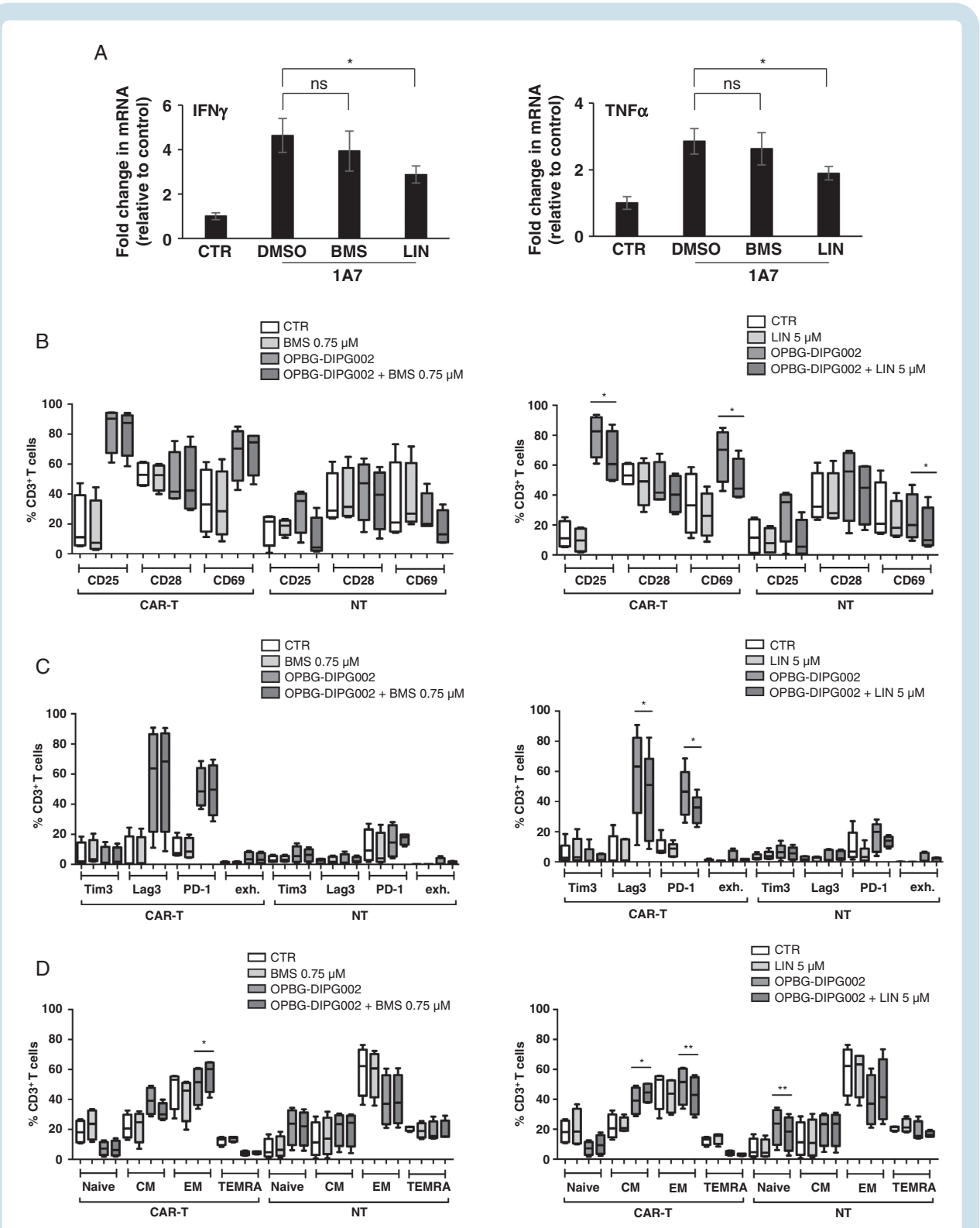

Fig. 4 Effect of BMS and LIN treatments on GD2-CAR T-cell phenotypes. (A) IFNα (*left panel*) and TNFγ (*right panel*) mRNA levels in 1A7-activated CAR-T cells treated with BMS, LIN, or DMSO as vehicle control. Data are normalized to the nonactivated CAR-T cells (CTR). Results are presented as mean ± SD of 3 independent repeats. (B–D) Box-plots representating activation (B), exhaustion (C), and memory (D) profiles of CAR or NT T-cells in coculture for 96 h with or without OPGB-DIPG002, in presence of LIN (*left panel*) or BMS (*right panel*). Results are presented as mean ± SD from 4 donors.

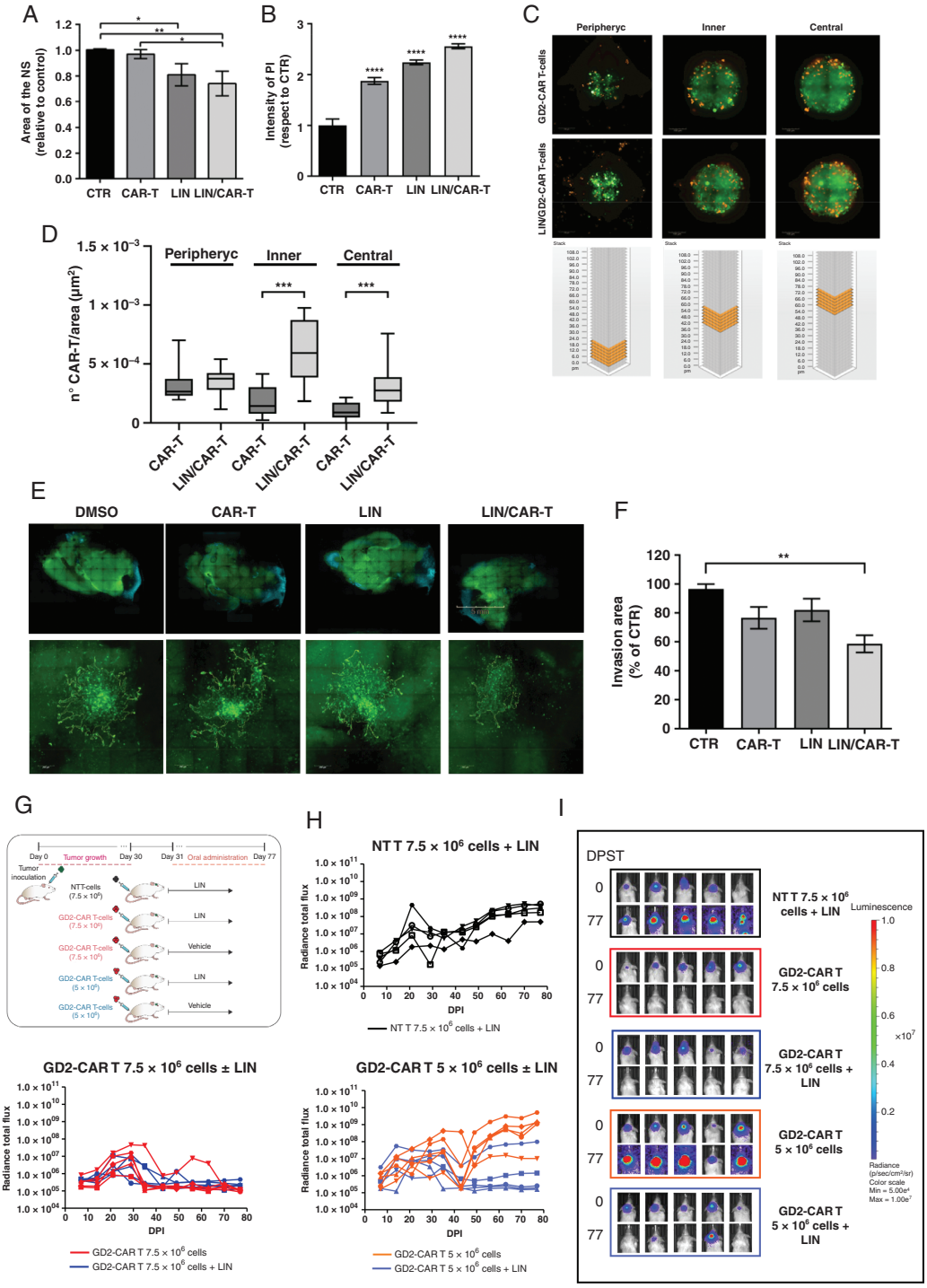

Fig. 5 Effect of LIN/GD2-CAR T-cells combination on DIPG 3D models in vitro, ex vivo, and in vivo. (A–B) SU-DIPG-VI-eGFP⁺ NS cocultured for 24 h ± CAR T-cells, in presence of LIN (5 µM) or DMSO as control. (A) Analysis of NS size and (B) PI staining intensity. Data are mean ± SD, $n = 3$. (C–D) Representative Z-stack fluorescent images (C) of SU-DIPG-VI-eGFP⁺ NS cocultured with CAR T-cells prelabeled with PKH26, in presence of LIN, or DMSO as control with schematic view of the Z-stack. The number of CAR-T cells identified in the different regions of the NS is shown (D). Data are mean ± SD, $n = 3$. (E–F) Mosaic images (10×, *upper panel*) of WBOS after spreading of SU-DIPG-VI-eGFP⁺ NS implanted in the pontine area. WBOS/DIPG cocultures were treated with DMSO, CAR T-cells, LIN (5 µM), or LIN/CAR T-cells (E). Tumor invasion area (40×, *lower panel, segmentation*) was quantified with ImageJ (F). Results are mean ± SD of $n = 3$. (G–I) Effect of LIN/GD2-CAR T-cells combination on SU-DIPG-VI-eGFP⁺/LUC⁺ orthotopic xenograft model in NSG mice. (G) Scheme of the experiment. (H) Bioluminescent image analysis of tumor growth is expressed as radiance total flux (p/s/cm²/sr) over days post implantation (DPI). (I) Images of the engrafted tumors evaluated at the indicated time points (5 mice/group).

vehicle control, and cocultured in the presence or absence of OPBG-DIPG002 cells for 96 h followed by flow-cytometry analysis. As expected, the T-cell activation markers CD25 and CD69, as well as the activation/exhaustion markers Lag3 and PD-1 were increased in GD2-CAR T-cells in the presence of OPBG-DIPG002 cells (Figure 4B and C). Also, in coculture with OPBG-DIPG002, a decrease in *naïve* and terminally differentiated along with an increase in central memory T-cells were observed within the CAR T-cell population (Figure 4D). The T-cell markers were modest or absent in the NT T-cells used as control for GD2-CAR specificity.

When CAR T-cells were in coculture with OPBG-DIPG002 and in presence of BMS, no variations in the expression of the different T-cell markers were observed compared to the same condition in absence of BMS (Figure 4B and C, left panel), with the only exception of a significant increase in the effector memory profile (Figure 4D, left panel).

However, when CAR T-cells where in coculture with OPBG-DIPG002 and in the presence of LIN, we detected a significant decrease in the expression of CD25 and CD69 (Figure 4B, right panel) as well as of PD-1 and Lag3 (Figure 4C, right panel), compared to the same condition in absence of LIN. In addition, we observed a significant reduction of T-cell maturation with an increase in central memory and a reduction of the effector memory (Figure 4D, right panel).

Altogether our results clearly indicate that both antagonists have different effects on T-cells. LIN remarkably decreases GD2-CAR T-cell exhaustion and induces a more T-cell immature phenotype. Since both characteristics have been reported to be essential for a better in vivo T-cell persistence phenotype, we selected LIN for further in vitro efficacy studies.

Anti-Tumor Activity of LIN/GD2-CAR T-Cells Combination Treatment in DIPG 3D Models, In Vitro and Ex Vivo

To further test the LIN/GD2-CAR T-cell combination in more complex culture models of DIPG, we used in vitro 3D neurospheres (NS) and ex vivo organotypic brain slice models.

In vitro, SU-DIPG-VI cells grown as NS and previously transduced to express eGFP (SU-DIPG-VI-eGFP$^+$) (Supplementary Figure 6), were cocultured for 24 h with or without GD2-CAR T-cells, either in presence or absence of LIN. When used as single agent, LIN, but not GD2-CAR T-cells, induced a significant reduction in NS size, compared to control. Instead, GD2-CAR T-cells affected the tight DIPG NS structure, which appeared more loose compared to control (Figure 5A and Supplementary Figure 7A). At the end of the incubation time, propidium iodide (PI) was added for cell death quantification. Both, LIN and GD2-CAR T-cells significantly induced tumor cell death compared to controls, as demonstrated by the increase in PI intensity, which was further enhanced when LIN/GD2-CAR T-cells were used in combination (Figure 5B and Supplementary Figure 7A).

Next, we analyzed the effect of LIN on the infiltrative properties of GD2-CAR T-cells. NS were cocultured with GD2-CAR T-cells prelabelled with PKH26 and treated as described above. Analysis of the maximal projection of Z-stack images from the pheripheric, inner, and central regions of the NS revealed that CAR T-cells had significantly infiltrated more deeply the NS in presence of LIN than in its absence (Figure 5B and Supplementary Figure 7B).

To mimic a more in vivo-like environment, SU-DIPG-VI-eGFP+ NS were implanted in the pontine region of whole brain organotypic brain slices and cocultured with or without GD2-CAR T-cells, in presence or absence of LIN (Figure 5E). Image analysis revealed that GD2-CAR T-cells and LIN partially inhibited DIPG invasion in comparison to the untreated control and that this effect was only significantly enhanced when the two agents were used in combination (Figure 5F), demonstrating the positive effect of LIN/GD2-CAR T-cell therapeutic strategy in an ex vivo model of DIPG.

Anti-Tumor Activity of LIN/GD2-CAR T-Cells Combination Treatment in Vivo

To confirm our combination strategy in vivo, we established an orthotopic xenograft model of DIPG by implanting the SU-DIPG-VI-eGFP+LUC+ cells in the pons of NSG mice. First, we defined the optimal treatment condition for both agents to observe a combinatorial effect. LIN was orally administered and tested in a dose escalating experiment with 12.5, 25, and 50 mg/kg in comparison to 25 mM tartaric acid used as vehicle control (Supplementary Figure 8A, C, and E). LIN was generally well tolerated; however, no anti-tumor activity was observed at any of the tested doses (Supplementary Figure 9A). For the GD2-CAR T-cells, we administered systemically 2.5×10^6, 5×10^6 or 10×10^6 cells, and 10×10^6 cells NT-T cells as control (Supplementary Figure 8B, D, and F). A strong and sustained reduction of the tumor burden was observed with 10×10^6 GD2-CAR T-cells. For both 5 and 2.5×10^6 CAR T-cells, an initial decrease followed by tumor re-growth was seen (Supplementary Figure 8D and F). Based on these data, we performed the combination study with mice treated with 7.5×10^6 GD2-CAR T-cells ± LIN, 5×10^6 GD2-CAR T-cells ± LIN and 7.5×10^6 NT T-cells ± LIN used as control. LIN was used at 50 mg/kg. LIN neither affected tumor growth of the NT T-cells treated cohort, nor improved the already sustained response obtained with 7.5×10^6 GD2-CAR T-cells. While in the 5×10^6 GD2-CAR T-cells treated mice only transient anti-tumor effect was observed with CAR-T alone, a sustained anti-tumor effect was found in presence of LIN (Figure 5D and Supplementary Figure S8), thus confirming the enhanced anti-tumor effect of our combination strategy in vivo.

Discussion

The recent preclinical demonstration of CAR T-cell efficacy in DMG H3K27M-mutant has provided the rationale for opening several clinical trials in this brain tumor (NCT04196413, NCT04099797, and NCT04185038).

Our observation that GD2 is not restricted to DMG H3K27M-mutant, but widely expressed in pHGGs

independently of location/histone molecular status, suggests that GD2-CAR T-cell therapy could be extended beyond the DMG H3K27M-mutant. However, GD2 staining appeared heterogeneous in terms of expression level and sub-cellular localization. While the IHC does not allow to clearly discriminate between cytoplasmic and membranous localization, the flow-cytometry analysis unequivocally showed GD2 expression on the membrane of our primary cell lines. In contrast to our IHC tissue findings, in the cell lines, as also reported by Mount et al.[11] we found that GD2 is detected only in H3K27M-mutant. We hypothesize that in vitro, where the cells are grown under stem cell-like conditions, GD2 expression is dependent on the H3K27M mutation, while, in vivo, the TME could drive GD2 expression independently of the histone status.

The heterogeneous GD2 expression we observe in patient tissues, together with the reported DMG H3K27M-mutant GD2^{low} cells could lead to an in vivo CAR T-cell treatment escape,[11] and the pHGGs and DMG immune-cold and/or immune-suppressive microenvironment,[26,27] led us to screen several compounds that, in combination with GD2-CAR T-cells, could improve their anti-tumor efficacy.

From the drug screening, we identified two dual IGF1R/IR antagonists as potent inhibitors of DIPG cell viability and potential adjuvants for GD2-CAR T-cell therapy. These inhibitors induce DIPG cell death through IGF1R/IR pathway inhibition, without affecting GD2-CAR T-cell viability.

The enhanced IGF1R/IR activity is known to support uncontrolled cell proliferation and the development of several malignancies, including brain tumors.[28,29] In pHGGs, IGF1R expression is associated with adverse outcome and radio-resistance.[30] Focal amplification in *IGF1R* gene with increase in its expression was demonstrated in DMG/DIPG.[2,14,31] Moreover, BMS was identified as a promising therapeutic agent in DMG/DIPG[25,32] and LIN was reported to be a strong inhibitor of DIPG cell proliferation in a 3D culture model.[33] These findings, together with ours, confirm the dependency of DIPG cells on the IGF1R/IR pathway for cell survival.

In addition, there is increasing evidence that IGF1R/IR pathways regulate the immune system by promoting an immunosuppressive and anti-inflammatory response within the TME.[34–36] For instance, IGF1 regulates the activation of cells endowed with immune-suppressive properties, such as regulatory T-cells[37] and promotes macrophage polarization from the pro-inflammatory M1 to the pro-tumorigenic M2 phenotype.[38] Therefore, IGF1R/IR pathway inhibition could contribute to reduce the immunomodulation displayed by the tumor environment, favoring CAR T-cell anti-tumor activity.

Although the GD2-CAR T-cells did not express IGF1R and IR, LIN and BMS treatment differentially affected their phenotypes, likely mediated through different off-target effects that remain to be identified. However, the action of LIN on the decrease in exhaustion and on the increase of less differentiated central memory T cells subpopulations, are features suggesting a better in vivo T-cell persistence.[39] Since less differentiated T cells are superior to effector T cells for adoptive cell therapy,[39] LIN appears more suitable as adjuvant for GD2-CAR T-cell therapy than BMS. Remarkably, the reduction of the other activation markers, namely CD25 and CD69, does not seem to correlate with an impairment of GD2-CAR T-cell activity. In addition, we observed that our CAR T-cells infiltrated more deeply into the NS in presence of LIN. While we cannot exclude a direct effect of LIN on the modulation of the intrinsic infiltrative property of the T cells, another explanation might be that in vitro LIN, by inducing tumor cell death, creates space allowing T cells to infiltrate further into the NS. Therefore, LIN treatment may present the double advantage to act by inducing DIPG cell death and by enhancing the persistence and tumor infiltration of the GD2-CAR T-cells. As a closer step to an in vivo pathophysiological condition, we established an ex vivo organotypic brain slice model of DIPG. In line with our in vitro data, the observed reduction of the DIPG cell invasion upon treatment with the combination therapy could be linked to tumor cell death. However, we cannot exclude effects on the invasive ability of these cells and/or other effects mediated by the microenvironment.

The dual IGF1R/IR antagonists have a poor ability to cross the blood–brain barrier (BBB), which limits preclinical studies for brain cancers.[25,32] To our knowledge, there is no published PK study demonstrating that LIN cross the BBB either in preclinical models and/or in patients. Our in vivo data with LIN as single agent, suggest that it does not penetrate in the brain, at least not at a dose sufficient to observe anti-tumor efficacy in our DIPG orthotopic xenograft model. A dedicated PK/PD study would need to be performed in the future to precisely assess the peak concentration of LIN in the brain in nontumor bearing versus tumor bearing mice before translating these results to the clinic. CAR T-cells are known to cross and disrupt the BBB,[40] therefore, it is possible to speculate that they may improve LIN permeability through the BBB when coadministered. Notably, the LIN/GD2-CAR T-cell treatment was effective using a lower CAR T-cell number when compared to the same used as single agent. Based on our in vitro data, it is likely that LIN, by improving CAR-T cell persistence and infiltration, prolongs and sustains their anti-tumor activity also in vivo. One aim of the combination therapy is to decrease the doses of CAR-T cells to limit their potential toxicity and still achieve potent anti-tumor efficacy. Our results in vivo are in line with this hypothesis, suggesting that our combination strategy should be able to reduce potential toxicity associated to CAR-T cell therapy.

In conclusion, our study provides strong evidence for the therapeutic potential of LIN/GD2-CAR T-cell combination strategy and supports the development of IGF1R/IR inhibitors to be used in combination with GD2-CAR T-cells for the treatment of DMG/DIPG H3K27M-mutant and potentially for other pHGG.

Supplementary Material

Supplementary material is available at *Neuro-Oncology* online.

Keywords

CAR T-cells | DIPG | DMG | IGF1R/IR | immunotherapy

Funding

This work was funded by Children with cancer UK Grant 16-234 (M.V.); DIPG Collaborative (M.V.); Fondazione Mia Neri (E.D.B.); Accelerator Award-Cancer Research UK/AIRC-INCAR project (F.L.); Fondazione AIRC per la Ricerca sul Cancro - Special Project 5x1000 no. 9962 (F.L.); Fondazione AIRC per la Ricerca sul Cancro IG 2018 id. 21724 (F.L.); Ministero dell'Università e della Ricerca Grant PRIN 2017 (F.L.); Italian Ministry of Health project on CAR T RCR-2019-23669115 (F.L.); Agenzia Italiana del Farmaco - Independent research grant PI: 2016 call (F.L.); Italian Ministry of Health Ricerca Finalizzata RF-2016-02364388 (F.L.); Italian Ministry of Health Ricerca Corrente (F.L., C.Q., B.D.A., I.C., M.V.); Italian Ministry of Health GR-2013-02359212 (C.Q.); Italian Ministry of Health GR-2016-02364546 (B.D.A.); Fondazione AIRC per la Ricerca sul Cancro Start-Up Grant, id.17184 (I.C.). We further acknowledge Fondazione Heal and Fondazione Umberto Veronesi (fellowship to M.P., R.F.). M.V. is a CwCUK Fellow.

Acknowledgments

We thank Professor Michelle Monje for providing SU-DIPG-VI cells.

Conflict of interest statement. The authors declare no conflict of interest.

Authorship statement. Concept and design: E.D.B., F.L., and M.V. Experiments and data collection: E.D.B., M.P., D.O., G.P., R.F., P.B., M.A.A.C., N.M., M.P., C.D.S., P.B., A.P., G.W., and S.C. Data analysis and interpretation: E.D.B., M.P., D.O., G.P., R.F., S.R., L.L.P., B.D.A., I.C., and Q.C. Reagents, cases, data and/or clinical annotation: S.R., F.D.C., R.R., L.M., C.J., A.C., B.D.A., I.C., Q.C., and A.M. E.D.B. and M.V. drafted and all authors reviewed and approved the final manuscript.

References

1. El-Khouly FE, Veldhuijzen van Zanten SEM, Santa-Maria Lopez V, et al. Diagnostics and treatment of diffuse intrinsic pontine glioma: where do we stand? *J Neurooncol*. 2019;145(11):177–184.
2. Mackay A, Burford A, Carvalho D, et al. Integrated molecular meta-analysis of 1,000 pediatric high-grade and diffuse intrinsic pontine glioma. *Cancer Cell*. 2017;32(4):520–537.e5.
3. Wu G, Broniscer A, McEachron TA, et al. Somatic histone H3 alterations in pediatric diffuse intrinsic pontine gliomas and non-brainstem glioblastomas. *Nat Genet*. 2012;44(3):251–253.
4. Schwartzentruber J, Korshunov A, Liu XY, et al. Driver mutations in histone H3.3 and chromatin remodelling genes in paediatric glioblastoma. *Nature*. 2012;482(7384):226–231.
5. Louis DN, Perry A, Reifenberger G, et al. The 2016 World Health Organization classification of tumors of the central nervous system: a summary. *Acta Neuropathol*. 2016;131(6):803–820.
6. Sievers P, Sill M, Schrimpf D, et al. A subset of pediatric-type thalamic gliomas share a distinct DNA methylation profile, H3K27me3 loss and frequent alteration of EGFR. *Neuro Oncol*. 2021;23(1):34–43.
7. Louis DN, Perry A, Wesseling P, et al. The 2021 WHO classification of tumors of the central nervous system: a summary. *Neuro Oncol*. 2021;23(8):1231–1251.
8. Janssens GO, Gandola L, Bolle S, et al. Survival benefit for patients with diffuse intrinsic pontine glioma (DIPG) undergoing re-irradiation at first progression: a matched-cohort analysis on behalf of the SIOP-E-HGG/DIPG working group. *Eur J Cancer*. 2017;73:38–47.
9. Rechberger JS, Lu VM, Zhang L, Power EA, Daniels DJ. Clinical trials for diffuse intrinsic pontine glioma: the current state of affairs. *Childs Nerv Syst*. 2020;36(1):39–46.
10. Vinci M, Burford A, Molinari V, et al. Functional diversity and cooperativity between subclonal populations of pediatric glioblastoma and diffuse intrinsic pontine glioma cells. *Nat Med*. 2018;24(8):1204–1215.
11. Mount CW, Majzner RG, Sundaresh S, et al. Potent antitumor efficacy of anti-GD2 CAR T cells in H3-K27M(+) diffuse midline gliomas. *Nat Med*. 2018;24(5):572–579.
12. Schuelke MR, Wongthida P, Thompson J, et al. Diverse immunotherapies can effectively treat syngeneic brainstem tumors in the absence of overt toxicity. *J Immunother Cancer*. 2019;7(1):188.
13. Majzner RG, Theruvath JL, Nellan A, et al. CAR T cells targeting B7-H3, a pan-cancer antigen, demonstrate potent preclinical activity against pediatric solid tumors and brain tumors. *Clin Cancer Res*. 2019;25(8):2560–2574.
14. Mackay A, Burford A, Molinari V, et al. Molecular, pathological, radiological, and immune profiling of non-brainstem pediatric high-grade glioma from the HERBY phase II randomized trial. *Cancer Cell*. 2018;33(5):829–842.e5.
15. Bonaventura P, Shekarian T, Alcazer V, et al. Cold tumors: a therapeutic challenge for immunotherapy. *Front Immunol*. 2019;10:168.
16. Quintarelli C, Orlando D, Boffa I, et al. Choice of costimulatory domains and of cytokines determines CAR T-cell activity in neuroblastoma. *Oncoimmunology*. 2018;7(6):e1433518.
17. Knochelmann HM, Smith AS, Dwyer CJ, Wyatt MM, Mehrotra S, Paulos CM. CAR T cells in solid tumors: blueprints for building effective therapies. *Front Immunol*. 2018;9:1740.
18. Ramello MC, Haura EB, Abate-Daga D. CAR-T cells and combination therapies: what's next in the immunotherapy revolution? *Pharmacol Res*. 2018;129:194–203.
19. Chrusciel E, Urban-Wojciuk Z, Arcimowicz L, et al. Adoptive cell therapy-harnessing antigen-specific T cells to target solid tumours. *Cancers (Basel)*. 2020;12(3):1–30.
20. Newick K, O'Brien S, Moon E, Albelda SM. CAR T cell therapy for solid tumors. *Annu Rev Med*. 2017;68:139–152.
21. Pericoli G, Petrini S, Giorda E, et al. Integration of multiple platforms for the analysis of multifluorescent marking technology applied to pediatric GBM and DIPG. *Int J Mol Sci* . 2020;2121(18):1–25.
22. Sen G, Chakraborty M, Foon KA, Reisfeld RA, Bhattacharya-Chatterjee MB. Induction of IgG antibodies by an anti-idiotype antibody mimicking disialoganglioside GD2. *J Immunother*. 1998;21(1):75–83.

23. Vera J, Savoldo B, Vigouroux S, et al. T lymphocytes redirected against the kappa light chain of human immunoglobulin efficiently kill mature B lymphocyte-derived malignant cells. *Blood*. 2006;108(12):3890–3897.
24. Marconi S, De Toni L, Lovato L, et al. Expression of gangliosides on glial and neuronal cells in normal and pathological adult human brain. *J Neuroimmunol*. 2005;170(1–2):115–121.
25. Halvorson KG, Barton KL, Schroeder K, et al. A high-throughput in vitro drug screen in a genetically engineered mouse model of diffuse intrinsic pontine glioma identifies BMS-754807 as a promising therapeutic agent. *PLoS One*. 2015;10(3):e0118926.
26. Lin GL, Nagaraja S, Filbin MG, Suva ML, Vogel H, Monje M. Non-inflammatory tumor microenvironment of diffuse intrinsic pontine glioma. *Acta Neuropathol Commun*. 2018;6(1):51.
27. Mi Y, Guo N, Luan J, et al. The emerging role of myeloid-derived suppressor cells in the glioma immune suppressive microenvironment. *Front Immunol*. 2020;11:737.
28. Gualco E, Wang JY, Del Valle L, et al. IGF-IR in neuroprotection and brain tumors. *Front Biosci (Landmark Ed)*. 2009;14:352–375.
29. Bielen A, Perryman L, Box GM, et al. Enhanced efficacy of IGF1R inhibition in pediatric glioblastoma by combinatorial targeting of PDGFRalpha/beta. *Mol Cancer Ther*. 2011;10(8):1407–1418.
30. Simpson AD, Soo YWJ, Rieunier G, et al. Type 1 IGF receptor associates with adverse outcome and cellular radioresistance in paediatric high-grade glioma. *Br J Cancer*. 2020;122(5):624–629.
31. Paugh BS, Broniscer A, Qu C, et al. Genome-wide analyses identify recurrent amplifications of receptor tyrosine kinases and cell-cycle regulatory genes in diffuse intrinsic pontine glioma. *J Clin Oncol*. 2011;29(30):3999–4006.
32. Lin GL, Wilson KM, Ceribelli M, et al. Therapeutic strategies for diffuse midline glioma from high-throughput combination drug screening. *Sci Transl Med*. 2019;11(519):1–16.
33. Meel MH, Sewing ACP, Waranecki P, et al. Culture methods of diffuse intrinsic pontine glioma cells determine response to targeted therapies. *Exp Cell Res*. 2017;360(2):397–403.
34. Hunt P, Eardley DD. Suppressive effects of insulin and insulin-like growth factor-1 (IGF1) on immune responses. *J Immunol*. 1986;136(11):3994–3999.
35. Yahya MA, Sharon SM, Hantisteanu S, Hallak M, Bruchim I. The role of the insulin-like growth factor 1 pathway in immune tumor microenvironment and its clinical ramifications in gynecologic malignancies. *Front Endocrinol (Lausanne)*. 2018;9:297.
36. Zhao Z, Zhang N, Li A, et al. Insulin-like growth factor-1 receptor induces immunosuppression in lung cancer by upregulating B7-H4 expression through the MEK/ERK signaling pathway. *Cancer Lett*. 2020;485:14–26.
37. Miyagawa I, Nakayamada S, Nakano K, et al. Induction of regulatory t cells and its regulation with insulin-like growth factor/insulin-like growth factor binding protein-4 by human mesenchymal stem cells. *J Immunol*. 2017;199(5):1616–1625.
38. Spadaro O, Camell CD, Bosurgi L, et al. IGF1 shapes macrophage activation in response to immunometabolic challenge. *Cell Rep*. 2017;19(2):225–234.
39. McLellan AD, Ali Hosseini Rad SM. Chimeric antigen receptor T cell persistence and memory cell formation. *Immunol Cell Biol*. 2019;97(7):664–674.
40. Gust J, Hay KA, Hanafi LA, et al. Endothelial activation and blood-brain barrier disruption in neurotoxicity after adoptive immunotherapy with CD19 CAR-T Cells. *Cancer Discov*. 2017;7(12):1404–1419.